Orientational Dependence of the Surface Free Energy of the $L_\alpha - L_3$ Interface

O. D. Lavrentovich,[†,‡] C. Quilliet,[†] and M. Kléman*[,†]

Laboratoire de Minéralogie-Cristallographie[§] T16, Case 115, Université Pierre-et-Marie-Curie, 4, Place Jussieu, F-75252 Paris Cédex 05, and Chemical Physics Program and Liquid Crystal Institute, Kent State University, Kent, Ohio, 44242

Received: August 30, 1996; In Final Form: October 22, 1996[⊗]

Geometrical, topological, and energetical properties on an interface between the lamellar L_α and the isotropic sponge phase L_3 are considered. The sponge phase shows a characteristic interbilayer separation d_3 that is larger than the interbilayer separation d_α in the L_α phase. This feature controls the experimentally observed phenomenon of orientational epitaxy (Quilliet, C.; Blanc, C.; Kléman, M. *Phys. Rev. Lett.* **1996**, *77*, 522) that keeps the lamellar L_α bilayers tilted with respect to the interface. We discuss the concentration profile near the interface, the geometry of smooth matching between the bilayers of both phases and estimate the surface tension of the $L_\alpha - L_3$ interface at equilibrium orientation of layers. The energy needed to deviate the layers from the equilibrium orientation ("anchoring" energy) is calculated using the Frenkel−Kontorova dislocation model. The model also predicts faceting, which is observed experimentally. Both the surface tension and anchoring energies are of the order of K/d_α, where K is the bend elastic constant. The role of layer undulation in tangential anchoring is discussed and illustrated experimentally. Finally, an outcome of the theory is that the orientation is related to the topological parameter of the sponge phase (coordination number of the passages introduced by Porte *et al., J. Phys. (Paris)* **1988**, *49*, 511).

1. Introduction

One of the interests of soft matter systems such as colloidal solutions of amphiphilic species is that the characteristic lengths are much higher than in the classical objects of solid state physics (between 10 to 100 nm). In particular, the order parameter variations through an interface between such systems are likely to occur on mesoscopic scales.

We present here a model for the interface between two phases of membranes: the lamellar L_α phase and the "sponge" L_3 phase, which are solutions of surfactants. The L_α phase is made of bilayers of surfactants, or membranes, separated by the solvent, with a repeat distance $d_\alpha = \delta + d_w$, where d_w is the thickness of the layer of solvent, and δ is the thickness of the membrane (Figure 1). It has a smetic A symmetry: liquid order in the membranes, and solid, or crystalline, order perpendicularly to the membranes. Its free energy density is written

$$f_\alpha = {}^1/_2\, K(\mathrm{div}\ \mathbf{n})^2 + {}^1/_2 B(\partial u/\partial \varsigma)^2 + \bar{K}\, g \qquad (1)$$

where u is the displacement of the bilayers measured along the axis ς perpendicular to the layers, B is the compression constant, K and $\bar{K}$ are the bend and saddle-splay smectic elastic constants, which respectively specify the energy cost of the mean and Gaussian curvature of the smectic. The unit normal to the layers is the director $\mathbf{n}$. We have div $\mathbf{n} = \pm(\sigma_1 + \sigma_2)$ of the order of $\pm(\partial^2 u/\partial x^2 + \partial^2 u/\partial y^2)$ if the curvatures are small, and $g = \sigma_1\sigma_2$; σ_1 and σ_2 are the principal curvatures of the layers.[1]

The L_3 or sponge phase is more complex; it is isotropic but birefringent under shear, and generally stable over a rather narrow range of compositions. There are probably several sponge phases, among them the "symmetric" and the "asymmetric" are clearly documented (see below). The L_3 phase we have in mind in the present theoretical work is the symmetric sponge phase, whose widely admitted model is as follows: it is made of a single bilayer without edges nor seams, separating the whole solvent into two *equivalent* entangled parts—hence the qualification of *symmetric* and *bicontinuous* given to this model of the sponge phase (Figure 1). This bilayer has a nontrivial topology, with many connections such as handles, or passages, and shows a zero average mean curvature and a negative average Gaussian curvature.[2,3] This phase has no positional nor orientational order; it features a typical interbilayer distance d_3 which has been put experimentally into evidence by X-ray and neutron small-angle scattering; d_3 does not correspond to a Bragg peak, of evidence, but to a bump in the intensity vs wave vector plot.[2] This distance d_3 is also acknowledged as being the characteristic size of passages or handles. We shall adopt the above model of the "symmetric" sponge phase.

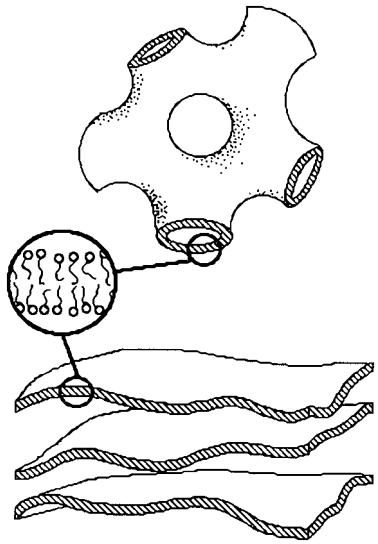

Figure 1. Approximate arrangement of surfactant bilayers in the sponge L_3 (above) and lamellar L_α (below) phases.

* Author to whom correspondence should be addressed.
† Université Pierre-et-Marie-Curie.
‡ Kent State University.
§ Unité de Recherche Associée 009 du CNRS, associée aux Universités de Paris VI et Paris VII.
⊗ Abstract published in *Advance ACS Abstracts,* December 15, 1996.

S1089-5647(96)02632-6 CCC: $14.00

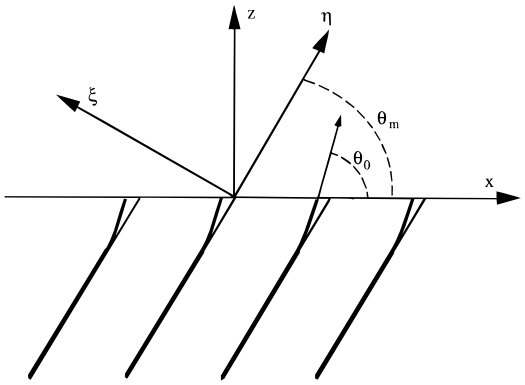

Figure 2. Definition of angles θ_m and θ_0 that the L_α bilayers make with the interface.

Experimental studies[4,5] revealed that there is a nontrivial tilt angle θ between the L_α bilayers and the $L_\alpha - L_3$ interface. The order of magnitude of this angle is consistent with the hypothesis of matching between the two characteristic distances d_α and d_3 of the two phases in contact. Nevertheless, by considering more accurately the data of Quilliet *et al.*,[5] we may observe a general tendency of the measured value θ_m of θ to be higher (by ~15%) than the value $\theta^* = \sin^{-1}(d_\alpha/d_3)$ calculated from the X-ray data and the epitaxial matching hypothesis. The hypothesis is nevertheless still consistent, when a modification of the characteristics of the L_3 phase near the interface is taken into account. This point is treated in section 2, utilizing a Landau−Ginzburg expansion type. In section 3, we present an estimation of the surface tension at the matching angle θ_m, and in section 4 we study how the surface energy changes when the bilayers deviate from the matching value, in the framework of a Frenkel−Kontorova model. In other words, we address smaller and smaller typical distances ξ when going from section 2 ($\xi \gg d_\alpha, d_3$) to sections 3 and 4 ($\xi \approx d_\alpha, d_3$). The results are then compared to experimental data.

2. Concentration Profile near the Interface

We are investigating the nature of the transition layer at the interface between the lamellar L_α and the L_3 sponge phase in a swollen surfactant. As stated above, we have experimental evidence[4,5] that the contact between the two phases at equilibrium, in the biphasic region, is of the "epitaxial" type, and is below any "roughening transition", so that the contact yields faceting.[6] The epitaxy is defined by the ratio $d_\alpha/d_3 = \sin\theta^*$. The optically measured tilt angle θ_m of the bilayers (Figure 2) is systematically larger than the X-ray deduced angle θ^*, and the following considerations will also tend to explain this.

The L_α and the L_3 phases in equilibrium do not have the same composition; the transition is obviously first order, as in any phase transition between multicomponents systems, generically. Therefore the surfactant volume fraction ϕ shows a jump $\phi_3 - \phi_\alpha$ when going from the L_α phase to the L_3 phase. However this cannot be so in the experimental situation: the surfactant bilayers must vary continuously through the transition layer, for obvious energetical and topological reasons; therefore, the solvent volume fraction also varies continuously from its value $\phi_\alpha = \phi_{z=-\infty}$ in the bulk of the L_α phase to its value $\phi_3 = \phi_{z=+\infty}$ in the bulk of the L_3 phase.

We analyze the transition region in two steps, first in the L_3 phase, second in the L_α phase. We assume a sharp transition at $z = 0$, and a smooth variation on both sides, in the L_3 phase for $z > 0$, in the L_α phase for $z < 0$.

In the L_3 phase, we adopt the Landau−Ginzburg free energy by adding a gradient term to the expansion due to Wennerström et al.,[7] viz.

$$f_3 = -t\phi^3 + v\phi^5 + w(\nabla\phi)^2 \tag{2}$$

where t, v, and w are positive elastic coefficients. We know that this expression of the free energy is controversial[8,9] in two respects: in the first place, as shown by Cates, Roux, *et al.*,[10,11] the thermal fluctuations of the membranes, which are well-known to renormalize the curvature moduli, yield a logarithmic term in the free energy (of the form $\delta f^3 = t'\phi^3 \ln \phi$), which can be dominant at very high dilutions, i.e., when the characteristic length d_3 (which is of the order of the distance between passages) is large, compared to the de Gennes−Taupin[12] persistence length $\xi = l_{mol} \exp 4\pi\kappa/k_BT$, where l_{mol} is a molecular length; in fact, the samples we have been investigating are well above this high dilution regime, and we can safely forget the logarithmic correction. In the second place, we do not know how the rigidity coefficient w scales with d_3; it might diverge for large dilutions; but again, we are not in a regime of high dilutions. We therefore adopt the Landau−Ginzburg free energy expansion in the form 2 above.

The Euler−Lagrange equation which minimizes the total energy $\int_0^\infty f_3\ (\phi, (\partial\phi/\partial z)\ dz$ is

$$2w(\partial^2\phi/\partial z^2) = -3t\phi^2 + 5v\phi^4 \tag{3}$$

and at equilibrium we have

$$3t = 5v\phi_\infty^2 \tag{4}$$

The positive z axis is along the outward normal to the L_α phase. Since $\phi_3 = \phi_\infty$ for z infinite, and $(\partial\phi/\partial z)_{z=\infty} = 0$, the first integral of eq 3 is

$$w(\partial\phi/\partial z)^2 = -t(\phi^3 - \phi_3^3) + v(\phi^5 - \phi_3^5) \tag{5}$$

which, using eq 4 and after some standard manipulation, can be written:

$$\begin{aligned} w(\partial\phi/\partial z)^2 &= {}^1/_3\, v[3\phi^3(\phi^2 - \phi_3^2) - 2\phi_3^2(\phi^3 - \phi_3^3)] \\ &= {}^1/_3 v(\phi - \phi_3)^2(2\phi_3^3 + 4\phi_3^2\phi + 6\phi_3\phi^2 + 3\phi^3) \end{aligned} \tag{6}$$

It is interesting to notice that the last member is always positive. Hence, this equation makes sense whatever the value of ϕ may be.

Let $\Phi = \phi - \phi_3$, we get

$$w(\partial\phi/\partial z)^2 = w(\partial\Phi/\partial z)^2 = 5v\phi_3^3\Phi^2 + O(\Phi^3) \tag{7}$$

Hence

$$\Phi = \Phi_0 \exp\left[-\sqrt{\frac{5v\phi_3{}^3}{w}}z\right] + \ldots \tag{8}$$

where $\Phi_0 = \phi_0 - \phi_3$.

Looking at orders of magnitude, let us introduce the sponge transition width $\Lambda_3 = \sqrt{5w/(v\phi_3{}^3)} \approx 2\bar{d}\phi_3^{-3/2}$, where $\bar{d} = \sqrt{w/v}$ is some material length (*at least* of the order of δ). Thus Λ_3 is large even when $\bar{d} \sim \delta$; in this case $\Lambda_3 \sim 2d_3\phi_3^{-1/2}$, since $d_3 = \mu(\delta/\phi)$, where μ is a numerical coefficient, of the order of 1.4, experimentally.[2] Taking $\phi_3 \approx 5/100$, $d_3 \approx 40$ nm, one gets $\Lambda_3 \approx 360$ nm.

What happens at the interface $z = 0$ deserves further comments. Let $d_{3;z=0}$ and $d_{\alpha;z=0}$ be the values of d_3 and d_α at the interface; we have

$$d_{3;z=0} = \frac{d_{\alpha;z=0}}{\sin\theta_0} = \mu_{z=0}\frac{\delta}{\phi_{3;z=0}} \tag{9}$$

where we have introduced the dimensionless variable $\mu(z)$, $\mu_{z=\infty} = \mu$ in the bulk. This variable is related to the coordination number of the passages.[2] Notice that, because of the continuity of ϕ at this boundary, which yields $\phi_0 = \phi_{3;z=0} \equiv \phi_{\alpha;z=0}$, the second equality in eq 9 can be written:

$$\mu_{z=0}\sin\theta_0 = 1, \tag{10}$$

since $d_{\alpha;z=0} = \delta/\phi_0$ (apart of logarithmic corrections, which are anyway small in the little swollen surfactants considered here). We shall show soon that θ_0 is close to θ_m. Hence, taking for the value of θ_0 the optically measured θ_m, we see that the coordination number Z at the boundary can be estimated directly from the experiment. We postpone to section 5 a more detailed discussion of the topological parameter μ.

The boundary $z = 0$ is a surface of continuity for ϕ, but a surface of discontinuity for the density of passages (which vanishes in the L_α phase) and for Z. As such, $z = 0$ can be considered as the boundary between the lamellar L_α phase and the sponge L_3 phase. In the L_α phase, we expect the lamellar layers to bend in order to react to the normal Ginzburg force on the L_3 side, relaxing from the value θ_0 near the interface to θ_m further in the bulk (Figure 2). A calculation given in the appendix shows that the relaxation length of the membranes deformation is of the order of $\Lambda_\alpha \approx \sqrt{d_\alpha\lambda/\pi}\sin\theta^*$, which is of the order of a characteristic length d_α in the L_α phase, i.e., much smaller than Λ_3. This calculation does not yield the value of θ_0 and θ_m directly; another relation is required, which states that the boundary is in mechanical equilibrium at $z = 0$:

$$\left.\frac{\delta f_3}{\delta z}\right|_{z=0} = \left.\frac{\delta f_\alpha}{\delta z}\right|_{z=0} \tag{11}$$

We expect $f_\alpha \approx B(\theta_0 - \theta_m)^2\exp(2z/\Lambda_\alpha) = B\Theta_0^2\exp(2z/\Lambda_\alpha)$ and $f_3 \approx -\varphi^3(k_BT/\delta^3)$. Since $\phi - \phi_3 = \Phi_0\exp(-z/\Lambda_3)$, eq 11 yields

$$\Theta_0^2/\Phi_0 \approx 3\phi_3^2\frac{k_BT}{\delta^3B}\frac{\Lambda_\alpha}{\Lambda_3} \approx 3\mu^2\frac{d_3}{\delta}\frac{\Lambda_\alpha}{\Lambda_3}$$

Hence, $\Theta_0 = \theta_0 - \theta_m$ is rather small; with $\mu = 1.4$, $d_3/\delta = 20$, $\Lambda_\alpha/\Lambda_3 = 1/10$, $\Phi_0 = \phi_3/100$, $\phi_3 = 5/100$, one gets $\phi_0 - \phi_m \approx 5^0$.

3. Microscopic Geometry of the L_α−L_3 Interface and Estimation of the Interfacial Tension

The interfacial energy is defined by an excess energy of healing of "free bonds" that are exposed when the two phases are cut and put in contact along the interfacial plane. Topology and energy of the interface strongly depend on the tilt angle θ between the L_α bilayers and the interface. In this section we analyze the case of matching, $\theta = \theta_m = \sin^{-1}(d_\alpha/d_{3,surf})$, where $d_{3,surf}$ is the periodicity of the surface layer of the L_3 phase (Figure 2). According to our discussion above (section 2), we have $d_{3,surf} = d_{3;z=0}$. For the sake of simplicity, we shall note this quantity d_3.

There are three basic geometries of healing: (a) with "edges" and "seams" (Figure 3a,b); (b) with "bridges" and "cups" (Figure 3c,d) and (c) with alternating "passages" and "bridges" (Figure 4). As we shall see below, it is the geometry (c) that results in likely the smallest energy of the interface and naturally provides the matching condition $\theta = \theta_m = \sin^{-1}(d_\alpha/d_3)$ for the tilted L_α bilayers.

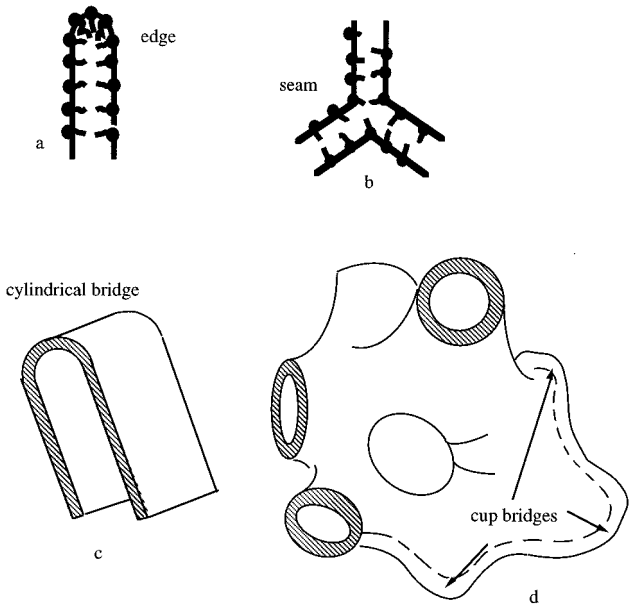

Figure 3. Healing of free bonds with an edge (a), seam (b), cup bridge (c), and cylindrical bridge (d).

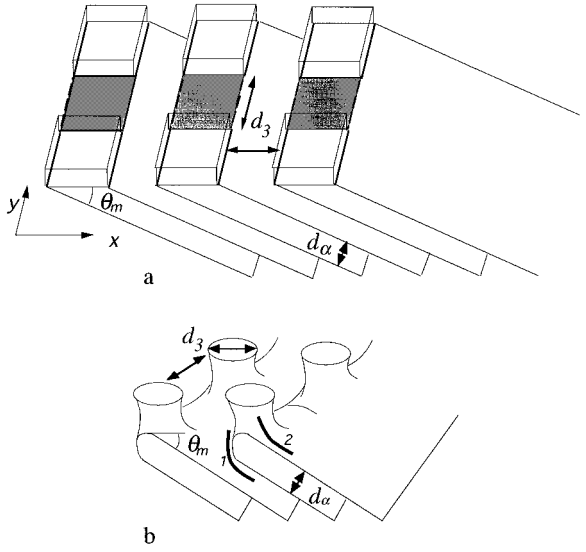

Figure 4. Matching structure of the L_3−L_α interface with continuous bilayers for the matching angle θ_m: (a) cubic model and (b) relaxed structure; local Gaussian curvature is positive in zone 1 and negative in zones 2.

(a) An edge of an individual bilayer and a seam (a junction of three bilayers) have molecular-scale curvatures $\sim 1/\delta$. The line energy is high,[2,13,14] of the order of κ_m/δ, where κ_m is the bending modulus of the monolayer. The surface energy of a unit area is then roughly $\sigma_{\alpha,e} \approx \kappa_m\sin|\theta|/\delta d_\alpha$ for the L_α side and $\sigma_{3,e} \approx \kappa_m/\delta d_3$ for the L_3 side.

(b) Bridges provide healing by connecting pairs of bilayers. A semicylindrical bridge (Figure 3c) that connects two neighboring L_α bilayers has a curvature $\sim 1/d_\alpha$ and line energy $\sim \kappa/d_\alpha$, where κ is the bending modulus of the bilayer. The interfacial energy per unit area of the L_α side is thus $\sigma_{\alpha,b} \approx \kappa\sin|\theta|/d_\alpha^2$. For the L_3 side, the analog of a bridge is a cup of positive Gaussian curvature $(2/d_3)^2$ that covers one L_3 passage (Figure 3d). The energy of one cup is $\sim (2\kappa + \bar{\kappa})$ and thus $\sigma_{3,b} \approx (2\kappa + \bar{\kappa})/d_3^2$; here $\bar{\kappa}$ is the Gaussian curvature elastic constant

for one bilayer ($\bar{\kappa} = \bar{K}d_\alpha$). Since the curvature of bridges and cups is smaller than that of edges and seams (especially for sufficiently diluted phases), $\sigma_{\alpha,b}$, $\sigma_{3,b} < \sigma_{\alpha,e}$, $\sigma_{3,e}$. Thus a realistic model of the $L_\alpha-L_3$ interface should operate with pairs of bilayers.

(c) To illustrate the most plausible geometry of healing with passages and bridges, one can first employ the cubic model of the sponge phase and the corresponding "square" model of the interface, in which the L_3 surface is represented by a set of squares with sides d_3, separated by distances d_3 (Figure 4a).

With the L_α bilayers tilted by the angle θ_m, all the edges of the L_3 squares, which are oriented along the axis *y*, are matching. These edges are shown by bold lines in Figure 4a. Nonmatching edges of squares (plain lines along the *x* axis) and nonmatching parts of L_α bilayers (dashed lines along the *y* axis) form a new set of squares shifted by distance d_3 with respect to the initial set. These squares can be filled with plaquettes of size $d_3 \times d_3$ (shadowed areas in Figure 4a). Obviously this arrangement with flat plaquettes will relax as in Figure 4b. The junctions between the L_3 passages and the L_α planes have partly positive Gaussian curvature (Figure 4b, zone 1) and partly negative one (Figure 4b, zone 2). The energy of the interface is likely to be a linear combination of κ and $\bar{\kappa}$. The above discussion suggests that κ enters in σ_m as $\sigma_m \approx a\kappa/d_3^2$ where $a \approx 1$ is a geometrical constant; the $\bar{\kappa}$ term can reduce the energy due to the presence of the passages; hence $\sigma_m \approx (a\kappa - c\bar{\kappa})/d_3^2$, where $c \approx 1$ is another geometrical constant. Near the $L_\alpha-L_3$ phase transition the saddle-splay constant $\bar{\kappa}$ is expected to be positive or, at least, close to zero.[3,15] Therefore, the surface tension σ_m of the interface is majored by $\sigma_m \approx a\kappa/d_3^2$. With $\kappa \approx k_BT$ and $d_3 =$ 40 nm, one gets $\sigma_m \approx 10^{-6}$ J/m^2 (10^{-3} erg/cm^2), i.e. a very small value. In principle, to this value two additional terms should be added, that come from the integration of the gradients of concentration and tilt over distances respectively Λ_3 and Λ_α. These two terms are of the order of $w\Phi_0^2/\Lambda_3$ and $B\Lambda_\alpha(\theta_0 - \theta_m)^2$, respectively. Since we found Λ_3 to be rather large and $(\theta_0 - \theta_m)$ to be rather small, we do not expect significant changes in the estimate of σ_m above.

In the following section we discuss what is the energy $W(\theta - \theta_m)$ needed to deviate the L_α lamellar bilayers from their equilibrium substrate-imposed tilted orientation; this quantity is often called "anchoring energy" in the physics of thermotropic liquid crystals, see, e.g., review by Blinov *et al.*[16]

4. Orientational-Dependent Part of the Interfacial Energy

The action of the L_3 substrate on the configuration of L_α bilayers can be modeled by a periodic potential U_3. In the "matching" state, $\theta = \theta_m = \sin^{-1}(d_\alpha/d_{3,surf})$, the L_α bilayers sit at the bottom of the U_3 potential troughs; in this section we will continue to denote $d_{3,surf}$ as d_3. The surface tension σ_m estimated above corresponds to the matching state. Any angular deviations ρ from $\theta = \theta_m$ should increase the interfacial energy. When $\rho \neq 0$, the spacing $d_\alpha/\sin(\theta_m + \rho) \approx d_3(1 - \rho \cot \theta_m)$ between the bilayers at the interface does not match d_3. In order to decrease the corresponding expense in the potential energy U_3, each bilayer has to displace toward the nearest minimum: this may induce some compression energy (the *B* term in eq 1).

The compression energy of the L_α bilayers can be easily derived if one considers the constraints imposed on the coordinates x_n and x_{n+1} of two neighboring bilayers by the change ρ in tilt. Obviously, the bilayers would remain unstrained when their separation $x_{n+1} - x_n = d_3 + \nu_{n+1} - \nu_n$ measured along the axis *x* is equal to $d_\alpha/\sin(\theta_m + \rho) \approx d_3(1 - \rho \cot\theta_m)$. Here ν_n and ν_{n+1} are, respectively, the displacements of the *n*-th and (*n*+1)-th bilayer from the corresponding bottoms of the troughs. Therefore, the derivative of the bilayers' displacement *u* along the bilayers' normal ς can be expressed as $\partial u/\partial\varsigma = (\partial\nu/\partial x) + \rho \cot\theta_m$ and the compression energy as $^1/_2B[(\partial\nu/\partial x) + \rho\cot\theta_m]^2$.

In fine, the equilibrium position and its global energy results from a balance between the potential energy and the compression energy. The problem formulated this way is reminiscent of the *Frenkel−Kontorova model* of a chain of identical particles connected by identical springs, subjected to a force which varies periodically along the chain.[17] A number of authors[18,19] have extended this model by allowing the nonconstrained period of the chain to be different from that of the substrate potential; this is the case we consider below.

If the interface is sufficiently long, the mismatch would create dislocations along the interface. When $|\rho| \ll 1$, the dislocations are well separated and the final surface energy includes the energy of a number *N* of dislocations (per unit length: $N|b| \sim |\rho|$, where **b** is the Burger's vector of the dislocation). For an isolated dislocation, the displacement ν would be changing from $\nu = 0$ at one end of the interface, say at $x \to -\infty$, to $\nu = \pm b$ at another end $x \to \infty$. We do not consider the case when $|\rho|$ becomes large enough to produce phenomena such as commensurate−incommensurate transitions (for a complete analysis of these, see the recent book by Chaikin and Lubensky[20]; the estimate of the critical $|\rho|$ (below which the model is valid for our system) is given below.

The energy of interface per unit length along the *y* axis can be thus written as the integral

$$U' = \int_{-\infty}^{\infty}\left[U_3(\nu) + {}^1/_2B\Lambda\left(\frac{d\nu}{dx} + \rho \cot \theta_m\right)^2\right]dx \qquad (12)$$

where $\nu = \nu(x)$ is the displacement field, Λ is the length along the *z* axis, on which the compression is effective (to be estimated below).

Since the quantity of interest is the difference *U* between the energy of the dislocated state and the energy of the dislocation-free state, then the ν-independent term $^1/_2B\Lambda\rho^2 \cot^2 \theta_m$ has to be subtracted from the integrand in eq 12:

$$U = \int_{-\infty}^{\infty}\left[U_3(\nu) + {}^1/_2B\Lambda\left(\frac{d\nu}{dx}\right)^2 + B\Lambda\rho\left(\frac{d\nu}{dx}\right)\cot \theta_m\right]dx \qquad (13)$$

The equilibrium arrangement of layers corresponds to the solution of the Euler−Lagrange equation for the functional (13):

$$B\Lambda\frac{d^2\nu}{dx^2} = \frac{\partial U_3}{\partial\nu} \qquad (14)$$

The first integral of eq 14 is of the form[20]

$$^1/_2B\Lambda\left(\frac{d\nu}{dx}\right)^2 = U_3(\nu) + \epsilon \qquad (15)$$

where ϵ is the constant of integration whose value should be determined by minimizing the energy *U* with respect to ϵ. It is easy to see what is the physical meaning of the particular value $\epsilon = 0$: the case $\epsilon = 0$ corresponds to noninteracting dislocations separated by infinitely large distances $L \to \infty$. Really, for the isolated dislocations the interfacial junctions between the L_α and L_3 bilayers far away from the dislocations cores are not disturbed; therefore, in the remote regions $d\nu/dx = 0$ and $U_3 = 0$ (the latter means that $\nu = 0, \pm b$). With these boundary conditions imposed, the first integral of eq 14 gives the result (15) with $\epsilon = 0$.

Physically, in our model of the $L_\alpha - L_3$ interface (which has no dislocations in the ground state), $\epsilon = 0$ corresponds to a small deviation $|\rho| \ll 1$ of the bilayers from an equilibrium orientation. Below, following Chaikin and Lubensky,[20] we estimate the critical value $|\rho_c|$ above which the ground state contains interacting dislocations separated by some finite equilibrium distance $L(\epsilon)$. We substitute eq 15 into eq 14 (taking into account different signs for positive and negative ρ) and use the idea that the displacement field $\nu(x)$ changes by the Burgers vector $\pm b$ when x changes by $\pm L$:

$$U = \frac{nd_3}{L}\left(\int_0^b \sqrt{2B\Lambda(U_3 + \epsilon)}\,d\nu - \epsilon L - B\Lambda b|\rho|\cot\theta_m\right) \quad (16)$$

where n is the total number of bilayers along the x axis. The equilibrium condition $\partial U/\partial\epsilon = 0$ has only two solutions:[20]

$$L^{-1} = 0$$

and

$$|\rho| = \frac{\tan\theta_m}{b}\int_0^b \sqrt{2(U_3 + \epsilon)/B\Lambda}\,d\nu$$

(when L is finite). The critical value $|\rho_c|$ above which the finite separation L between the dislocations becomes energetically preferable, is thus

$$|\rho_c| = \frac{\tan\theta_m}{b}\int_0^b \sqrt{2U_3/B\Lambda}\,d\nu \quad (17)$$

As we will see below, the average value of $\sqrt{2U_3/B\Lambda}$ is likely to be of the order of 0.1−1, thus the critcal tilt $|\rho_c|$ is large, of the order of tens of degrees. Since we are primarily interested in small deviations from the equilibrium, $|\rho| < |\rho_c|$, we can proceed with a simple case of independent dislocations and $\epsilon = 0$.

The (positive) energy $W(\rho)$ per unit area needed to deviate the bilayers from the equilibrium $\theta = \theta_m$ by a small angle $|\rho| \ll 1$ is therefore defined as $W(\rho) = \sigma - \sigma_m = U_d/L = U_d|\rho|\cot\theta_m/d_3$, where U_d is the energy per unit length of one isolated dislocation. We use $\epsilon = 0$ in eqs 13 and 15, and take into account different signs of the derivative $\partial\nu/\partial x$ for $\rho > 0$ and $\rho < 0$ to find first the energy per unit length of one dislocation:

$$U_d = \int_0^L \left[B\Lambda\left(\frac{d\nu}{dx}\right)^2 + B\Lambda\rho\cot\theta_m\frac{d\nu}{dx}\right]dx = \int_0^b \sqrt{2B\Lambda U_3}\,d\nu - |\rho|bB\Lambda\cot\theta_m \quad (18)$$

and then the ρ-dependent part of the interfacial energy that scales as $|\rho|$:

$$W(\rho) = \sqrt{\frac{2B\Lambda}{d_3}}|\rho|\cot\theta_m\int_0^b \sqrt{U_3(\nu)}\,d\nu + O(\rho^2) \quad (19)$$

To estimate the absolute value of the anchoring energy coefficient

$$W_a = \frac{\sqrt{2B\Lambda}}{d_3}\cot\theta_m\int_0^b \sqrt{U_3(\nu)}\,d\nu \quad (20)$$

one has to specify the periodic potential U_3 that models the action of the sponge substrate as well as Λ.

The periodic potential U_3 can be taken sinusoidally:

$$U_3(\nu) = U_0\left(1 - \cos\frac{2\pi\nu}{P_3}\right) \quad (21)$$

with period P_3 and amplitude U_0. Below we discuss the possible values of P_3 and U_0.

P_3 is directly related to the surface value of d_3. At first sight, one can choose $P_3 = d_3$. If $P_3 = d_3$, then the Burgers vector of the dislocation considered above must be taken as $b = \pm P_3 = \pm d_3$: Frenkel−Kontorova model above does not allow dislocations other than the elementary ones with $b = \pm P_3 = \pm d_3$. For example, there are no solutions with double Burgers vector $b = \pm 2P_3$, which is easy to verify by calculating the equilibrium displacement field $\nu(x)$ for an isolated dislocation using eq 15 with $\epsilon = 0$ and the explicit potential (eq 21):

$$\nu = \frac{2P_3}{\pi}\tan^{-1}\left[\tan\frac{\pi b}{4P_3}\exp\left[\pm\frac{2\pi}{P_3}\sqrt{\frac{U_0}{B\Lambda}}\left(x - \frac{L}{2}\right)\right]\right] \quad (22)$$

where the dislocation center is located at $x = L/2$: the coefficient $\tan(\pi b/4P_3)$ eliminates solutions $b = \pm 2P3$. On the other hand, topological peculiarities make $b = \pm 2d_3$ dislocations energetically preferable over the dislocations $b = \pm d_3$, as discussed in section 3. In fact, the junctions between the pairs of bilayers and the smoothly connected L_3 handles have a periodicity $P_3 = 2d_3$, as it is clear from Figure 4. Therefore the periodicity of the potential U_3 should be set as $P_3 = 2d_3$. With $P_3 = 2d_3$, the dislocations $b = \pm P_3 = \pm 2d_3$ represent an elementary dislocation for which the above calculations within the Frenkel−Kontorova model are justified.

The amplitude U_0 can be estimated as the energy of elastic reshaping of the L_3 handles when a bilayer is displaced from the minimum of U_3. The reshaping is due to the necessary continuity of the bilayer between the L_α and L_3 phases. Hence U_0 is strongly related to the elasticity of the L_3 phase. We do not know much about this latter, but it is likely to scale as $K/d_3 = \kappa/d_3^2$ per unit area. The saddle-splay constant does not enter U_0 as soon as the shifts of the neighboring bilayers are nearly equal and topology of the handles is preserved. In the core of the dislocations the topology is broken and the $\bar{K}$ contribution might be nonzero; one can include this contribution into the "core energy" of the defect.

With $P_3 = 2d_3$ and $U_0 \approx K/d_3$, one gets for the energy per unit length of dislocation line

$$U_d \approx \frac{8}{\pi}\sqrt{BK\Lambda d_3} + O(\rho) \quad (23)$$

We can test the validity of this latter result by using the results of the smectic elastic theory.[21] In smectics, the lateral extension (here in ς direction) of the dislocation core of Burger's vector **b** is $2b^2/\lambda$. We can compare this quantity with the characteristic length in the Frenkel−Kontorova dislocation over which the displacement changes by $\pm b$; as follows from eq 22, this length is approximately $l = 2d_3\sqrt{B\Lambda/U_0}$ (numerical calculations using eq 22 show that ν changes by $\pm 0.95 \times b$ over the interval l defined as above). This comparison provides $\Lambda \sim 10d_\alpha$ which is an upper estimate, since Λ is of the order of the relaxation length $\Lambda_\alpha \approx d_\alpha$ calculated in the appendix. Note that U_0 somehow smaller than K/d_3 taken above, would allow $\Lambda \approx \Lambda_\alpha \approx d_\alpha$. In any case, although the exact solution $\nu(x)$ can be obtained only numerically in a discrete model, it is clear that for $|\rho| \ll 1$ both the exact and the continuum solutions preserve the dependence $W(\rho) \approx |\rho|$; their difference is expected only

in the energy of the dislocation core where $d\nu/dx$ is large; even here, however, the exact results should not depart in the order of magnitude from the ones found above.

Now we are in the position to estimate the anchoring coefficient in the continuum model as

$$W_a \approx \frac{8}{\pi}\sqrt{\frac{BK\Lambda}{d_3}}\cot\theta_m \approx (1 \div 10)\frac{\kappa}{d_\alpha^2} \approx (1 \div 10)\sigma_m \quad (24)$$

which is rather large, $W_a \approx (10^{-6}-10^{-5})$ J/m^2 with typical estimates $\kappa \approx k_BT$ and $d_\alpha = (20-40)$ nm.

Note in conclusion that the dislocation contribution to the $L_\alpha - L_3$ interface energy is similar to the anchoring energy of the interface between a thermotropic smectic A phase and a homeotropically treated wall.[22,23] In both cases it is the layered structure which makes the leading term in the surface energy nonanalytic ($W(\rho) \approx |\rho|$) and large: the anchoring coefficient $\sim K/d_\alpha$ in eq 24 can be compared to the value $\approx K/l_{mol}$ experimentally found in thermotropic smectic A far from the smectic-nematic transition.[23] An important difference is that the lamellar bilayers at the $L_\alpha - L_3$ interface can have nontrivial (and large) tilt θ_m imposed by the peculiar structure of the sponge phase.

5. Discussion and Comparison with Experiments

Nucleation and Shape of L_α Droplets. Let us briefly summarize experimental findings on nucleating L_α droplets in an L_3 sponge matrix[4,5] which reveal a phenomenon of orientational epitaxy at the $L_\alpha - L_3$ interface. The tilt angle θ_m is close to the value $\theta = \sin^{-1}(d_\alpha/d_3)$ expected from the hypothesis that the layers are tilted to match the characteristic distances d_α and $d_3 > d_\alpha$ in the two phases. The shape of the droplets of 10−100 μm size is highly nonspherical and show either cylindrical[4,5] or more complex logarithmic spiral[5] profiles. The logarithmic spiral droplets have a concentric spherical packing of L_α bilayers. Larger droplets are more spherical; however, their boundaries are made of curved surface regions; the inner structure contains many defects that are hard to decipher.

The free energy of the L_α droplet of radius R that nucleates in the sponge matrix is defined by the condensation energy gain $\sim \Delta f R^3 < 0$ (Δf is the bulk energy density difference between the L_α and L_3 phases), the elastic energy $\sim \kappa R/d_\alpha > 0$ of possible bend deformations (see the discussions below), the surface tension energy $\sim \sigma_m R^2 > 0$ and the surface anchoring energy $\sim W(\rho)R^2 > 0$. We restrict our consideration to the case where R is large enough to provoke spontaneous growth; it is apparently the case for the droplets studied experimentally.[4,5]

The surface tension estimated in section 3 is rather small, $\sigma_m \approx \kappa/d_\alpha^2 \approx 10^{-6}$ J/m^2, if compared to surface tensions at other isotropic-liquid crystal interfaces (for example, it is about 10^{-5} J/m^2 for the thermotropic nematic-isotropic interface[24]. The smallness of σ_m is natural in our model of matching since the layers preserve continuity when crossing the interface, see Figure 4.

Despite the smallness of σ_m, the surface energy term definitely overweighs the elastic energy term for $R \gg d_\alpha$, since the latter generally scales as $\kappa R/d_\alpha$; the ratio of the surface-to-elastic bulk energy is thus of the order of R/d_α. The smallness of the elastic term precisely implies that the layers have the shape of Dupin cyclides, see the review by Boltenhagen *et al.*[25] Among these are spheres and focal conic domains. Spherical packing of layers is observed in logarithmic spiral droplets of radius 10−100 μm. Thus the elastic energy of these dropets scales as R, as follows from eq 1. In larger L_α droplets, one experimentally observes numerous focal conic domains; these droplets are reminiscent of thermotropic smectic droplets where spherical and generic focal conic domains form a well-established hierarchy[26,27] controlled by the balance of the surface and elastic bulk energy.[28,29] One might worry if the elastic energy of large L_α droplets with numerous defects could overweigh the surface energy. Although we do not know the exact configuration of layers in large droplets with multiple defects, this is unlikely: the family of focal conic domains forms a fractal object whose energy scales as R^m, where the exponent m is still substantially smaller than 2.[30] On the other hand, elastic bend energy can influence the size of the smallest domains in the droplet, at scales where the bulk and surface contributions are comparable.[28] Because of the estimates above, for the L_α phase we expect this scale to be small, of the order of d_α.

With elastic energy negligibly small for $R \gg d_\alpha$, the shape of the L_α droplets filled with Dupin cyclides is defined by the balance of the two surface terms, the "isotropic" surface tension $\sigma_m(\theta = \theta_m)$ and the "anisotropic" anchoring energy $W(\theta - \theta_m)$. If the anchoring were weak, $W \ll \sigma_m$, then the droplet would adopt a shape close to a spherical one. However, as the Frenkel−Kontorova model suggests, the anchoring coefficient is large, $W_a/\sigma_m \approx 1 \div 10$. As a result, the L_α droplet shape is nonspherical to allow the surface orientation of L_α bilayers to be as close to $\theta = \theta_m$ as possible over the whole interface. With $W_a/\sigma_m \sim 1 \div 10$, angular deviations $|\rho| = |\theta - \theta_m| > 0.1$ rad on extended portions of the surface are unlikely.

The situation is reminiscent of the phenomenon of faceting known for solid crystals. In both cases the underlying mechanism is the presence of cusps $W(\rho) \approx |\rho|$ in the surface energy function[20] and of a large value of the coefficient W_a. The faceting in L_α phase features two important differences as compared to the solid crystals. First, because of the one-dimensional positional order, the facets of the lamellar "monocrystals" take the shape of conical surfaces of revolution. Second, since the bend energy is small, the inner structure can be highly bent. One can imagine that small nucleating droplets are in the shape of spherical layers enveloping a nucleation site (for example, a dust particle). When such a droplet grows, it preserves the concentric spherical packing since the transformation into a set of flat bilayers requires topological changes (e.g., one has to drill out a cone to unfold the concentric layers) with high elastic and anchoring energy penalties. With spherical packing preserved, the surface adopts a logarithmic spiral "faceting" with $\theta = \theta_m$ and $\sigma = \sigma_m$ for concentric layers crossing the interface. Although the logarithmic spiral geometry does not provide the absolute minimum of the surface energy (e.g., conically shaped droplets with flat layers of the same volume are of smaller surface area[5], it is stable over long duration of observations.[5] Experiments[5] also show that angular deviations from $\theta = \theta_m$ are small: $|\rho| < 0.1$ over more than 90% of the total surface area, which agrees with the estimates of W_a/σ_m above.

Tangential Anchoring. In the limiting case of tangential anchoring, $\theta = 0$, the L_α bilayers are parallel to the interface and thus avoid crossing it. The interfacial region can be composed, for example, of passages connecting the sponge bulk to the L_α bilayer that is the closest to the interface; similarly, the L_3 passages can be covered with cup-bridges shown in Figure 3d. The curvature contribution $a'\kappa/d_3^2$ to the interfacial energy $\sigma_{||}$ is of the order of $\sigma_m \approx a\kappa/d_3^2$ estimated in section 3 for the matching case, or even smaller than σ_m. However, for tangential anchoring there is another contribution to the interfacial energy $\sigma_{||}$. The L_α bilayers that run parallel to the interface are subject to alternating attractive and repulsive forces set by the L_3 structure and thus experience an undulating action of the type

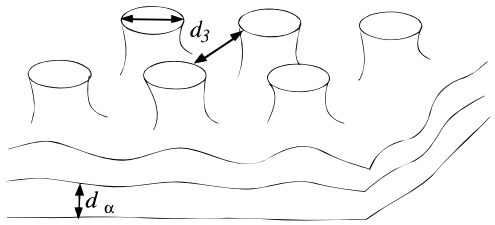

Figure 5. Undulation of lamellar bilayers at the $L_\alpha - L_3$ interface with tangential anchoring.

$u = u_0 \cos(\pi x/d_3)$ with amplitude $u_0 \sim d_\alpha$ (Figure 5). A classical calculation in smectics elasticity[1,31] shows that there would be a contribution to a surface energy $\sigma_{||}$ that scales approximately as $\kappa/d_\alpha\lambda$. Obviously this effect of undulations would vanish when the layers have quasiperpendicular (perpendicular or highly tilted) orientation at the interface.

The relative stability of parallel or quasiperpendicular anchoring of the lamellar layers on the $L_\alpha - L_3$ interface will depend on the relative values of the curvature $a'\kappa/d_3^2$ and undulation $\kappa/d_\alpha\lambda$ energies. A large λ value would induce preferentially a parallel anchoring, while for a "harder" lamellar phase with small λ, a tilted anchoring would be easier.

In view of this possibility, it is interesting to observe the behavior of a lamellar phase in which λ can be tuned. A good candidate is the ferrosmectic system, a quaternary mixture SDS/pentanol/water, whose swelling solvent is composed of cyclohexane with a suspension of magnetic nanoparticles. When only the magnetic particles volumic fraction ϕ_p in the swelling solvent is increased, then λ decreases while d_α[32] and κ[33] remain constant. Moreover, this system presents a $L_\alpha - L_3$ phase transition when increasing temperature, which allows us to observe L_α droplets into the sponge L_3 phase as in refs 4 and 5 and provides information on the tilt angle θ_m. Figure 6 shows such droplets in two systems that differ only by their solid particles contents. In Figure 6a the droplets are spherical with a concentric spherical packing of bilayers: the anchoring is planar. These droplets have been obtained in a system of low global magnetic particles volume fraction ϕ_p; the smectic penetration length λ of the lamellar part is then large. Figure 6b in contrast shows what happens in a system where λ is small and ϕ_p large: the droplets are anisotropic, which is characteristic of a quasiperpendicular orientation[4,6,26,34] and large anchoring coefficient. These features are then consistent with the tendencies discussed above.

Topology of the Bulk and Interface. The above model of matching of tilted layers implies a smooth transition between topologically different phases. Spatially changing topology falls within a broader circle of problems related to the role of the topological parameter μ in the $L_\alpha - L_3$ transition. Our consideration in section 2 suggests that its surface value $\mu_{z=0}$ can be estimated experimentally from the data on θ_m, as $\mu_{z=0} \approx \mu_{z=0,m} \equiv 1/\sin\theta_m$, see eq 10. In Figure 7, $\mu_{z=0,m}$ is plotted as a function of weight percentage of brine P_{br}, not much different from $(1 - \phi) \times 100$, with data reported by Quilliet *et al.*[5] It turns out that $\mu_{z=0,m}$ is slightly smaller than the bulk value.[32] According to Porte *et al.*,[2] μ relates in some way to the coordination number Z of the passages in an ideal "cubic" model; the Scherk surface yields $Z = 6$, i.e. $\mu \approx Z/4 = 1.5$: the sponge phase has seemingly a coordination number close to 6. A smaller value $\mu < 1.5$ means a smaller coordination number. Intuition goes the same direction as the experimental result which states that μ decreases when one gets closer to the interface: the coordination number vanishes in the L_α phase, and we expect that in the sponge phase Z should decrease monotonically through the transition region. For instance, $\theta_0 = 60°$, $\sin\theta_0 = 0.87$ (close to experimental values) yields $Z \approx 2.31$.

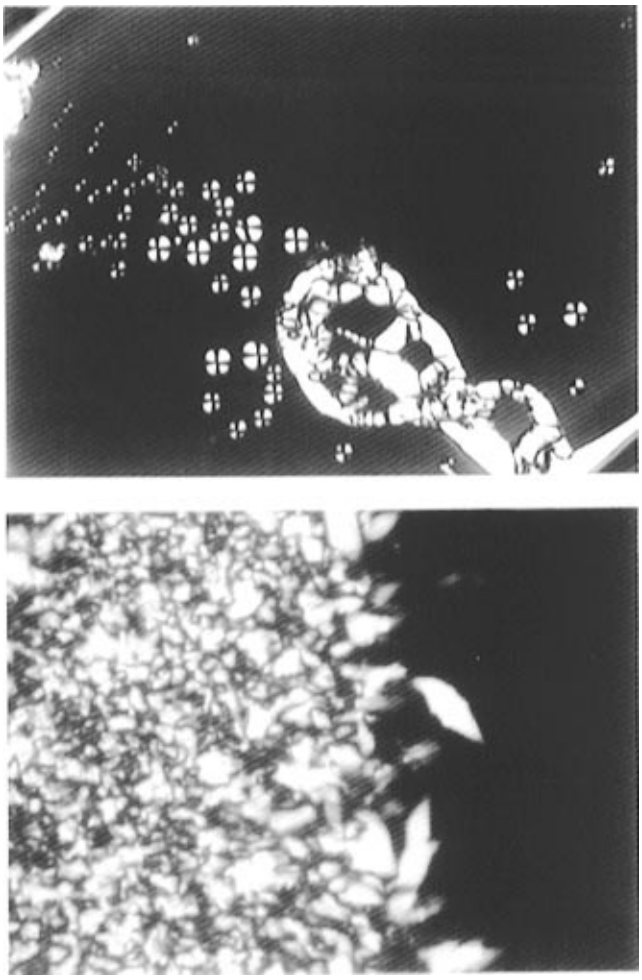

Figure 6. Polarizing optical microscopy observation of birefringent L_α droplets of a ferrosmectic in the isotropic sponge phase L_3, at T ≈ 50 °C, of a quaternary mixture of sodium dodecyl sulfate (SDS) 4.6% weight/pentanol 4% weight/water 11.6% weight/swelling solvent: suspension of magnetic particles in cyclohexane, 79.8% weight. (a, top) $\phi_p \approx 0.008$; (b, bottom) $\phi_p \approx 0.023$; ϕ_p = volume fraction of particles in cyclohexane.

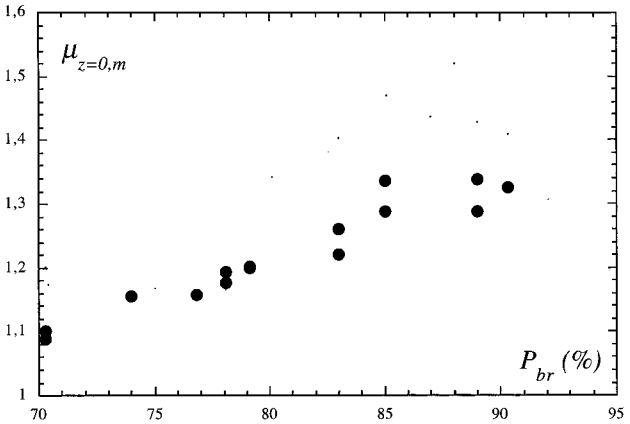

Figure 7. Plot of $\mu_{z=0,m} = 1/\sin\theta_m$ vs P_{br}.

Another interesting feature of Figure 7 is that $\mu_{z=0,m}$ changes with ϕ: $\mu_{z=0,m}$ is approximately 1.1 for the larger values of ϕ (≥ 0.2), and approximately 1.3 for the smaller ϕ's, which might indicate that there is some difference in the sponge phase structure for the two regimes of dilution. Other experiments carried on the same system ref 35, ref 36 (measurements of birefringence under shear), and ref 37 (detailed phase diagram) also reveal two types of sponge phase. Measurements show that in the more dilute samples $\phi < 0.2$ the birefringence scales

as expected in the usual model of the "symmetric" sponge phase (i.e. as ϕ^{-2} [38]). The less dilute samples, $\phi > 0.2$, show a different behavior.[36] All the above theoretical considerations in this article, in particular the study of the concentration profile, section 2, were based on the symmetric sponge phase model. Note that a spontaneous symmetry breaking of the symmetric sponge to an "asymmetric" sponge phase, where the two media of solvent are not equivalent, has been predicted[14] on general grounds and experimentally observed[39] in a system different from ours.

6. Conclusion

The phenomenon of orientational epitaxy at the $L_\alpha-L_3$ interface is an interesting example of anchoring behavior in liquid crystal systems and deserves further studies. On the experimental part, freeze−fracture studies are planned in order to verify the epitaxial phenomenon and matching continuous geometry of layers depicted in Figure 4. Hoffmann *et al.*[6] have published remarkable freeze−fracture microphotographs of flat interfaces with tilted L_α bilayers for the $L_\alpha-L_3$ biphasic region; although they do not mention the phenomenon of orientational epitaxy, their results give additional support to the idea of matching. Other geometries of matching might include twist boundaries suggested by Thomas *et al.*[40] for lamellar block copolymers. Extended studies of ferrosmectic systems subject to the magnetic field would also be of importance: first, for direct measurements of the surface tension; second, for producing field-oriented L_α "monocrystals" with faceting at equilibrium. Theoretically, it would be interesting to clarify how the topological parameter μ behaves during the $L_\alpha-L_3$ phase transition, across the $L_\alpha-L_3$ interface and with changing ϕ. The adequate form of the relevant free energy expansion with gradient terms for broad range of concentrations also remains a problem to solve.

Acknowledgment. We thank P. G. de Gennes for relevant remarks and K. McGrath and E. Raphaël for useful discussions. O.D.L. thanks Laboratoire de Minéralogie-Cristallographie, CNRS, KSU and NSF (ALCOM grant DMR 89-20147) for support.

Appendix

Figure 2 represents the coordinates at the $z = 0$ boundary. The contact angle is θ_0, but since the transition layer is of mesoscopic size, i.e. not recognizable with the polarizing light microscopy, the measured quantity is θ_m. The equilibrium equation of the smectic layers, observed at a scale larger than d_3, i.e. in a continuous model, is

$$\lambda^2\frac{\partial^4 u}{\partial\eta^4} = \frac{\partial^2 u}{\partial\xi^2} \tag{A1}$$

where $\lambda^2 = K/B$ is the penetration length squared, and u the layers displacement, measured along the ξ axis, and periodic along the x direction, with period $d_{3;z=0} = 2\pi/q$. Let $u = (S + iT)\exp iqx + c.c.$, where S and T are the functions of z alone. Equation A1 reads

$$(\Lambda + i\Theta)(S + iT)\exp iqx + c.c. = 0, \tag{A2}$$

where Λ and Θ are operators acting on S and T only. It is a long, but easy calculation, to show that

$$(\Lambda + i\Theta) = [\lambda(p\sin\theta_m + iq\cos\theta_m)^2 - p\cos\theta_m + iq\sin\theta_m][\lambda(p\sin\theta_m + iq\cos\theta_m)^2 + p\cos\theta_m - iq\sin\theta_m] \tag{A3}$$

where $p = d/dz$ is acting on S and T. Clearly, the solutions of eq A1 are of the form $u = \sum_k u_k \exp p_k z \times \exp iqx + c.c.$, where p_k's are the eigenvalues of the operator p. To see the nature of the solution it is enough to consider the solutions obtained by equating to zero only one of the four factors which enter in $\Lambda^2 + \Theta^2 = (\Lambda + i\Theta)(\Lambda - i\Theta)$. The first factor in eq A3, for example, has solutions

$$p = \frac{\cos\theta_m - 2i\lambda q\sin\theta_m\cos\theta_m \pm \sqrt{\cos^2\theta_m - 4i\lambda q\sin\theta_m}}{2\lambda\sin^2\theta_m} \tag{A4}$$

which display two lengths of relaxation and two periodicities. We are interested in the relaxation lengths. Let

$$\bar{\omega} = \sqrt{\frac{\cos^2\theta_m - 4i\lambda q\sin\theta_m}{2\lambda\sin^2\theta_m}} \tag{A5}$$

and ψ be the argument of the complex number $\bar{\omega}$, such that $\cos^2\theta_m - 4i\lambda q\sin\theta_m = (\cos^4\theta_m + 16\lambda^2q^2\sin^2\theta_m)^{1/2} \times \exp(-i\psi)$, i.e. $\tan\psi = 4\lambda q\sin\theta_m/\cos^2\theta_m$. The real part $\mathbf{R}\bar{\omega}$ reads

$$\mathbf{R}\bar{\omega} = \frac{\cos\theta_m\cos\psi/2}{2\lambda\cos^{1/2}\psi\sin^2\theta_m} = \frac{\cos\theta_m}{2\lambda\sin^2\theta_m}\sqrt{\frac{1+\cos\psi}{2\cos\psi}} \tag{A6}$$

Hence

$$\mathbf{R}p = \frac{\cos\theta_m}{2\lambda\sin^2\theta_m}\left[1 \pm \sqrt{\frac{1+\cos\psi}{2\cos\psi}}\right] = \frac{\cos\theta_m}{2\lambda\sin^2\theta_m}\left[1 \pm \sqrt{\frac{1+\sqrt{1+\tan^2\psi}}{2}}\right] \tag{A7}$$

Now, to look at orders of magnitude, we introduce in the equations above the bulk values of d_3 and d_α instead of the exact values at the interface:

$$1 + \tan^2\psi = \frac{\cos^4\theta_m + 16\lambda^2q^2\sin^2\theta_m}{\cos^4\theta_m} \approx \frac{(d_3^{\,2} - d_\alpha^{\,2})^2 + 64\pi^2\lambda^2 d_\alpha^{\,2}}{(d_3^{\,2} - d_\alpha^{\,2})^2} \tag{A8}$$

This quantity is not much different from $(64\pi^2\lambda^2d_\alpha^2)/(d_3^2 - d_\alpha^2)^2$, since $(d_3^2 - d_\alpha^2)$ is small compared to $8\pi\lambda d_\alpha$. Within the same approximation, it is large compared to unity, and we eventually find

$$\mathbf{R}p \approx \left(\frac{\pi d_3^{\,2}}{\lambda d_\alpha^{\,3}}\right)^{1/2} \tag{A9}$$

This result assumes that the periodicity of perturbations at the interface is d_3; with a periodicity taken twice as large, as in section 3, one would get $\mathbf{R}p \approx (\pi d_3^2/2\lambda d_\alpha^3)^{1/2}$

The conclusion is that the relaxation length $\mathbf{R}p^{-1} \approx \sin\theta^* (d_\alpha\lambda/\pi)^{1/2}$ is of the order of the characteristic distances in the two phases, hence much smaller than the width Λ of the transition region. The angle θ of the bilayers relaxes elastically on the relatively short distance $\mathbf{R}p^{-1}$ to its bulk value θ_m, which cannot be significantly different from θ_0. On the other hand, the bilayers suffer an undulation of small amplitude, but of large periodicity $\mathbf{Im}p^{-1}$. We have:

$$\mathbf{Im}p = \frac{q}{\sin\theta_m}\left[-2\cos\theta_m \pm \frac{1}{\cos\theta_m}\sqrt{\frac{2}{1+\sqrt{1+\tan^2\psi}}}\right] \quad \text{(A10)}$$

Hence, within the same approximation as above,

$$\mathbf{Im}p^{-1} \approx \sin\theta^* \sqrt{\frac{d_\alpha\lambda}{\pi}}$$

of the same order of magnitude as $\mathbf{R}p^{-1}$.

References and Notes

(1) de Gennes, P. G.; Prost, J. *The Physics of Liquid Crystals*; Clarendon Press: Oxford, 1993; Chapter 7.

(2) Porte, G.; Marignan, J.; Bassereau, P.; May, P. *J. Phys. (Paris)* **1988**, *49*. 511.

(3) Porte, G.; Appell, J.; Bassereau, P.; Marignan, J. *J. Phys. (Paris)* **1989**, *50*, 1335.

(4) Quilliet, C.; Kléman, M.; Benillouche, M.; Kalb, F. *C. R. Acad. Sci. Paris, Ser II* **1994**, *319*, 1469.

(5) Quilliet, C.; Blanc, C.; Kléman, M. *Phys. Rev. Lett.* **1996**, *77*, 522.

(6) Hoffmann, H.; Thunig, C.; Munkert, U.; Meyer, H. W.; Richter, W. *Langmuir* **1992**, *8*, 2629.

(7) Wennerström, H.; Olsson, U. *Langmuir* **1993**, *9*, 365. Daicic, J.; Olsson, U.; Wennerström, H.; Jerke, G.; Schurtenberger, P. *J. Phys. II* **1995**, *5*, 199; *Phys. Rev. E.* **1995**, *52*, 3266.

(8) Roux, D.; Nallet, F.; Coulon, C.; Cates, M. E. *J. Phys. II* **1996**, *6*, 91.

(9) Daicic, J.; Olsson, U.; Wennerström, H.; Jerke, G.; Schurtenberger, P. *J. Phys. II* **1996**, *6*, 95.

(10) Cates, M. E.; Roux, D.; Andelman, D.; Milner, S.; Safran, S. *Europhys. Lett.* **1988**, *5*, 733.

(11) Roux, D.; Coulon, C.; Cates, M. E. *J. Phys. Chem.* **1992**, *11*, 4174.

(12) de Gennes, P. G.; Taupin, C. *J. Phys. Chem.* **1982**, *86*, 2294.

(13) Filali, M.; Porte, G.; Appell, J.; Pfeuty, P. *J. Phys. II* **1994**, *4*, 349.

(14) Huse, D. A.; Leibler, S. *Phys. Rev. Lett.* **1991**, *66*, 437.

(15) Boltenhagen, P.; Lavrentovich, O.; Kléman, M. *J. Phys. II* **1991**, *1*, 1233; *Phys. Rev. A* **1992**, *46*, R1743.

(16) Blinov, L. M.; Kats, E. I.; Sonin, A. A. *Usp. Fiz. Nauk* **1987**, *152*, 449; *Sov. Phys. Usp.* **1987**, *30*, 604.

(17) Kontorova, T. A.; Frenkel, Ya. I. *Zh. Eksp. Teor. Fiz. (USSR)* **1938**, *8*, 89, 1340.

(18) Frank, F. C.; van der Merwe, J. H. *Proc. R. Soc.* **1949**, *A198*, 205; 216.

(19) Kochendörfer, A.; Seeger, A. *Z. Phys.* **1950**, *27*, 533.

(20) Chaikin, P. M.; Lubensky, T. C. *Principles of Condensed Matter Physics*; Cambridge University Press: Cambridge, 1995; Chapter 10.

(21) Kléman, M. *Liquid Crystals* **1988**, *3*, 1355.

(22) Durand, G. *Liq. Cryst.* **1993**, *14*, 159; Lebedev, V. V.; Muratov, A. R. *Zh. Eksp. Teor, Fiz.* **1993**, *103*, 2048; *JETP* **1993**, *76*, 1018.

(23) Li, Z.; Lavrentovich, O. D. *Phys. Rev. Lett.* **1994**, *73*, 280.

(24) Park, C. S.; Clark, N. A.; Noble, R. D. *Phys. Rev. Lett.* **1994**, *72*, 1838.

(25) Boltenhagen, P.; Kléman, M.; Lavrentovich, O. D. In *Soft Order in Physical Systems*; Eds. Rabin, Y., Bruinsma, R., Eds; Plenum: New York, 1994; p 5.

(26) Friedel, G. *Ann. Phys. (Paris)* **1922**, *18*, 237.

(27) Sethna, J. P.; Kléman, M. *Phys. Rev. A* **1982**, *26*, 3037.

(28) Lavrentovich, O. D. *Zh. Eksp. Teor. Fiz.* **1986**, *91*, 1666; *Sov. Phys. JETP* **1986**, *64*, 984; *Mol. Cryst. Liq. Cryst.* **1987**, *151*, 417.

(29) Fournier, J.-B.; Durand, G. *J. Phys. II* **1991**, *1*, 845.

(30) Bidaux, R.; Boccara, N.; Sarma, G.; de Sèze, L.; de Gennes, P. G.; Parodi, O. *J. Phys. (Paris)* **1973**, *34*, 661.

(31) Durand, G. *C. R. Acad. Sci. Paris, Sér. B* **1972**, *275*, 629.

(32) Quilliet, C.; Fabre, P.; Veyssié, M. *J. Phys. II* **1993**, *3*, 1371.

(33) Ponsinet, V.; Fabre, P. *J. Phys. Chem.* **1996**, *100*, 5035.

(34) Fournier, J.-B.; Warenghem, M.; Durand, G. *Phys. Rev. E* **1993**, *47*, 1144.

(35) The measurements of μ in the bulk show that it changes from approximately 1.2 at $\phi < 0.2$ to approximately 1.4 at $\phi > 0.2$ (C. Quillet, unpublished results).

(36) Mahjoub, H. F.; Tassin, J. F.; Kéman, M. In preparation.

(37) McGrath, K. M. In preparation.

(38) Mahjoub, H. F.; McGrath, K. M.; Kléman, M. *Langmuir* **1996**, *12*, 3131.

(39) Roux, D.; Cates, M. E.; Olsson, U.; Ball, R. C.; Nallet, F.; Bellocq, A. M. *Europhys. Lett.* **1990**, *11*, 229.

(40) Thomas, E. L.; Reffner, J. R.; Bellare, J. *J. Phys. (Paris), Suppl. Collect. Phys. C7* **1990**, *51*, C7−363. Carvalho, B. L.; Thomas, E. L. *Phys. Rev. Lett.* **1994**, *73*, 3321.